PREPARED FOR THE U.S. DEPARTMENT OF ENERGY,
UNDER CONTRACT DE-AC02-76CH03073

PPPL-3883rev
UC-70

PPPL-3883rev

Effect of Gas Fueling Location on H-mode Access in NSTX

by

R. Maingi, M. Bell, R. Bell, T. Biewer, C. Bush, C.S. Chang, D. Gates,
S. Kaye, H. Kugel, B. LeBlanc, R. Maqueda, J. Menard, D.Mueller,
R. Raman, S. Sabbagh, V. Soukhanovskii, and the NSTX Team

Revised April 2004

PRINCETON PLASMA
PHYSICS LABORATORY

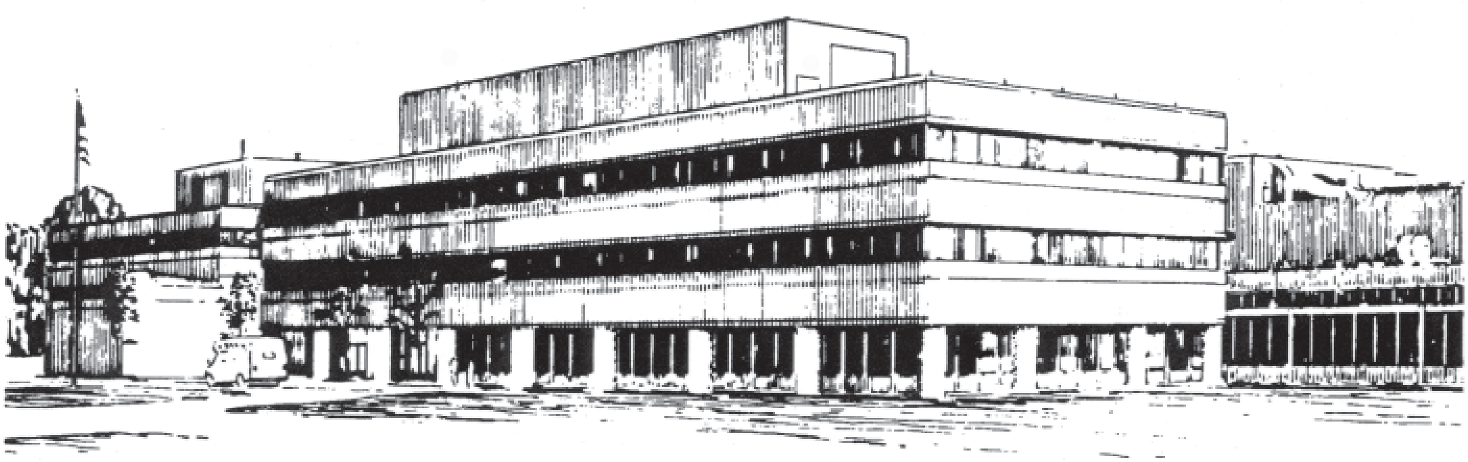

PRINCETON PLASMA PHYSICS LABORATORY
PRINCETON UNIVERSITY, PRINCETON, NEW JERSEY

Effect of Gas Fueling Location on H-mode Access in NSTX

R. Maingi[a], C.S. Chang[b,c], Seunghoe Ku[c], M. Bell[d], R. Bell[d], T. Biewer[d], C. Bush[a], D. Gates[d], S. Kaye[d], H. Kugel[d], B. LeBlanc[d], R. Maqueda[e], J. Menard[d], D. Mueller[d], R. Raman[f], S. Sabbagh[g], V. Soukhanovskii[h], and the NSTX Team

[a] *Oak Ridge National Laboratory, PO Box 2009, Oak Ridge TN, 37831, USA*
[b] *New York University, New York NY, USA*
[c] *Dept. of Physics, Korea Advanced Institute of Science and Technology, Daejon, Korea*
[d] *Princeton Plasma Physics Laboratory, PO Box 451, Princeton, NJ 08543, USA**
[e] *Los Alamos National Laboratory Los Alamos, NM, USA*
[f] *University of Washington, Seattle, WA USA*
[g] *Columbia University, New York, NY USA*
[h] *Lawrence Livermore National Laboratory, Livermore CA USA*

* correspondence address
first author email: rmaingi@pppl.gov
Submitted 07-Oct-2003

Abstract – *The dependence of H-mode access on the poloidal location of the gas injection source has been investigated in NSTX. We find that gas fueling from the center stack midplane area produces the most reproducible H-mode access with generally the lowest L-H threshold power in lower single-null configuration. The edge toroidal rotation velocity of C2+ is largest (in direction of the plasma current) just before the L-H transition with center stack midplane fueling, and then reverses direction after the L-H transition. Simulation of these results with a guiding center Monte Carlo neoclassical transport code (XGC) is qualitatively consistent with the trends in the measured velocities. Double-null discharges exhibit H-mode access with gas fueling from either the center stack midplane or center stack top locations, indicating a reduced sensitivity of H-mode access on fueling location in that shape.*

PACs: 52.55Fa

It has been previously reported that in both MAST[1] and NSTX[2], fueling from the center stack region (i.e. high-field side, HFS) allowed more reproducible H-mode access than fueling from the outer midplane or other low-field side (LFS) locations. Quantifying this behavior in NSTX has been challenging, however. Prior to HFS fueling, it was difficult to obtain routine H-modes with LFS fueling in NSTX. In contrast, long reproducible H-modes were obtained during the first attempt with HFS fueling following the first high temperature (~350 ^{0}C) bake-out of the graphite plasma facing surfaces. We note that HFS gas fueling widened[3] the H-mode access space and reduced the power threshold somewhat in COMPASS-D, as compared with LFS fueling. Reported experiments with fueling poloidal location variations have been minimal from conventional aspect ratio tokamaks. We not that HFS fueling was about twice as efficient as LFS fueling during DIII-D ELMy H-modes[4], although the gross fueling efficiencies were less than 1% in both cases. However in the NSTX discharges reported here, we found that the fueling efficiencies were comparable.

The present H-mode access scenario in NSTX uses LFS fueling for the gas pre-fill before t=0 and during the current ramp up prior to neutral beam initiation, which typically starts at t~0.1 sec. The LFS injection is usually terminated just before NBI turn-on, when HFS fueling is initiated. Due to the long tube used for HFS midplane injection, the e-folding decay time of the flow rate[5] is ~ 0.55 sec, resulting in limited control of the fueling rate.

Motivated by these and other experimental results, a neoclassical transport theory revision was developed[6,7 and references therein] to examine the dependence of the momentum balance on the poloidal location of the gas injection source. The theory applies to the edge plasma within the neutral penetration depth from the last closed flux surface where the neutral concentration is in the range from 10^{-4} to 10^{-3}. This theory predicts that a spontaneous toroidal rotation in the counter plasma current direction will be observed in the absence of other momentum sources. With other momentum source (e.g. neutral beams), a rotation in the direction of the momentum source will be established. The rotation originating from the external torque is also strongly dependent on the poloidal location of fueling. The theory suggests that the charge-exchange viscous drag is higher for neutral sources on the LFS than the HFS, because the ions lost to charge exchange have the highest toroidal velocity (v_ϕ) at the weakest toroidal field (B_ϕ) point, i.e. the outer midplane. As a result, both the v_ϕ and radial electric field (E_r) have terms with $1/R_*^2$ (in fact the rotation from external torque has an $1/R_*^4$ term) where R_* is the major radius at which gas fuels the plasma. This effect should be most apparent in a spherical torus because it features the largest variations in R_* from the inner to outer midplane, e.g. for NSTX $R_* \sim 7.5$.

Additional gas injectors at various poloidal locations were commissioned in NSTX to test this prediction and improve gas fueling control. Fig. 1 shows the four injector locations: HFS midplane (black), HFS top in upper corner (orange), outer midplane (blue), and lower X-point region (white). These injectors were used to fuel routine lower-single-null, upper-single null, and double-null discharges with plasma current I_P ~ 0.9 MA, toroidal field B_t ~ 0.45 T, and 3.2 MW of neutral beam injected (NBI) power. The unfiltered light patterns from these discharges showed localized emission near the gas injector locations in the HFS fueling discharges in lower-single null configuration, and somewhat more diffuse fueling in double-null configuration and also with LFS fueling (see Fig. 2). Most of this visible light originates from D_α recycling light, suggesting that the neutral density poloidal variation is affected by the choice of puff location. We do not quantify this variation in this paper, but merely use it as an indicator the neutral density poloidal distribution can be modified to qualitatively test the neoclassical theory prediction above.

The first three injectors were each used to fuel a lower-single null discharge during the neutral beam injection (NBI) phase, e.g. starting at t=0.08 sec in Fig. 3. Prior to NBI (the pre-fill and during plasma current ramp-up), all of the gas fueling was injected with a separate outboard injector. The total gas input during NBI was well matched in the three cases, and the time dependence of the gas injection rate was reasonably well matched. In all three cases the line-average density at 0.243sec (i.e. the last Thomson scattering point before the L-H transition time from the HFS midplane discharges) was 2.3 X 10^{19} m^{-3}, proving that that the fueling efficiency was similar from these injectors. In addition the n_e, T_e and P_e radial profiles were nearly identical for all of these discharges at that time. However the HFS midplane injector discharge (black trace) exhibited H-mode access at t=0.255 sec, whereas the other two discharges with LFS and HFS top fueling exhibited prolonged L-modes and early reconnection events.

Note that the reconnection time (t=0.260 sec) for the LFS fueled discharge in fig. 3 is, unfortunately, very close to the time of the transition for the HFS midplane discharge; other LFS fueled discharges which avoided the reconnection for a longer time also did not exhibit an H-mode transition, but were missing edge rotation data, necessitating the use of the present LFS fueled discharge. We note that the other HFS midplane discharges in this configuration exhibited H-mode transitions from 0.252-255sec, suggesting that the discharge-to-discharge variations in wall conditions which can affect the time of the L-H transition, were minimal. For completeness, we refer the reader to an overview[8] of the NSTX wall conditioning program.

This experiment was conducted near the beginning of the 2003 run period, when the L-H transition power was between one and two NBI sources, i.e. higher than normal threshold levels. We previously reported [2] that the LFS injector only produced H-mode access at an NBI power between 1.6 and 3.2 MW (between 1 and 2 sources) in conditions[9] where the L-H threshold power was measured at ~ 650 kW with HFS midplane fueling, i.e. below 1 full NBI source. In that set of experiments, the required NBI power for H-mode access became similar between the two fueling locations as the gas rate was reduced, but the reproducibility was still better with the HFS midplane injector. Here poor reproducibility means that H-mode access was achieved only on the first of two successive identically programmed LFS fueled discharges. In those discharges, the transition occurred earlier in time (at t=180ms about 10ms after I_p flattop), and the line density at the transition was 2.0 X 10^{19} m^{-3}. The lower limit on fueling rate was set by the occurrence of locked modes with either injector. At very high fueling rates (line density > 2.8 X 10^{19} m^{-3}), the H-mode could not be accessed at all with LFS gas puffing, even though access was maintained with the HFS midplane injector. These observations imply that the neutral density magnitude itself likely affects H-mode access criteria. Finally we note that fueling with a combination of the X-point injector and LFS injector failed to produce H-mode transitions despite obtaining similar line density of 2.4 X 10^{19} m^{-3} at t=0.25sec, the approximate time when the transition was observed in the HFS midplane fueled discharges.

Fig. 4 compares the magnitude of the edge toroidal rotation for the discharges from Fig. 3. The edge rotation speed for the HFS midplane discharge is marginally but consistently higher (co-I_p with co-NBI, reproducible in other discharges from this experiment) than for the other fueling locations just before the time of the L-H transition of the HFS midplane fueled discharges. The statistical error bar magnitude (plotted e.g. for the HFS discharge) is smaller than the size of the symbol, and the location of peak emission relative to the separatrix just before the L-H transition was the same in these discharges (we note, however, that larger variations in the signal can be observed later in time due to plasma temporal evolution). It was clear that the LFS and HFS top fueling cases failed to access H-mode and resulted in shorter discharges (see Fig. 3). The edge rotation velocity is obtained from Abel-inversions of passive edge rotation signals of C-

III light [10]. The diagnostic has a ~ 3cm edge spatial resolution and integrates over 10msec. The rotation velocity at the radius of peak emission (R~1.48m, normalized poloidal flux ψ_N ~ 0.95-0.99, depending on time slice and magnetic mapping) is plotted, because it has the lowest statistical and inversion errors. This mapping places the measurement location in a range from the density pedestal top to approximately the middle of the steep gradient region of where the pedestal forms e.g. in the HFS discharge with the L-H transition. Unfortunately the poloidal rotation array was unavailable during this experiment, precluding a statement on the effect of fueling location on E_r in this paper.

In double-null discharges, the differences between fueling from the HFS midplane and HFS top were more subtle. Discharges fueled by either injector allowed H-mode access at comparable power levels; the major difference was the location of the D_α fueling light, which was centered about the midplane for midplane fueling and near the upper corner for top fueling (fig. 2).

We have simulated the effect of neutral source poloidal location variation in the lower-single null configuration with a new Monte Carlo guiding center code (XGC)[11] with neoclassical and/or anomalous cross-field transport in an X-point geometry. XGC follows the guiding center particles in 3-D real space using a well-known Hamiltonian guiding center equation of motion [12], but the electrostatic potential is assumed to be a flux function and solved in 2-D space. The poloidal distribution of the neutral fueling source is a Gaussian plus a baseline as a function of the poloidal angle, θ. The location of the peak of the Gaussian is selected to match the fueling location. The ratio of the maximum fueling source of the Gaussian to the baseline value is set (somewhat arbitrarily at a high value for exploration) to 50. The integral of the fueling source term (in effect, the maximum of the Gaussian) is constrained by the input edge density value through recycling. The model edge temperature and heat input at the inner most radius is constrained by the input experiment value, and the anomalous cross-field diffusion coefficients are selected to approximately match the density and temperature profiles. The neutral beam momentum source was omitted for simplicity; a proper inclusion of the source would result in a positive offset to the toroidal rotation relative to the ones computed here. Hence the relative response (i.e. the sign and magnitude of the change) of the edge rotation to the fueling source location is the quantity of interest. Three simulations were conducted: one of the LFS midplane fueled L-mode phase, one of the HFS midplane fueled L-mode phase, and one of the HFS midplane fueled H-mode phase after the L-H transition. An anomalous cross-field diffusion coefficient of 2 m^2/s was used to model the L-mode phases, which was then reduced to 0.1 m^2/s for modeling of the H-mode phase.

Fig. 5 shows that the flux surface averaged main ion toroidal rotation in the experimentally relevant radii is predicted to be higher for the HFS midplane fueling than the LFS fueling cases, consistent with the analytic theory [6]. The toroidal rotation is in the co-I_p direction. Fig. 6 shows that the co-I_p edge toroidal rotation is predicted to be reduced in the H-mode phase, and sharply turns to negative direction close to the separatrix due to the larger negative E_r in the H-mode phase. Both of these code observations are consistent with the above experimental observations.

In general a co-I_p toroidal rotation is driven by the negative radial pressure gradient force (mostly density gradient force in banana-plateau regime [13]), and a counter-I_p rotation is driven by the negative E_r force. From the numerical simulation, we find that the E_r force, when compared with the radial pressure gradient force, becomes significant close to the separatrix only. In the absence of the neutral beam momentum input, the co-I_p toroidal rotation away from the separatrix observed in Figures 5 and 6 is, thus, driven by the dominance of the radial density and temperature gradient force over the radial E_r force. However, close to the separatrix, the negative E_r induced by the edge effects (radial orbit excursion and neutral effects) is dominant and turns the toroidal rotation toward negative direction.

We submit that the difference in the toroidal rotation speed between the HFS and LFS fueling originates from multiple neutral particle effects. The direct neutral effect discussed in Ref. [6,7] will make the positive toroidal rotation smaller for LFS fueling. This effect is magnified by the fact that the computed neutral penetration is somewhat deeper with LFS fueling due to the outboard flux compression. Additionally, this deeper neutral penetration with LFS fueling makes the ambient L-mode density gradient weaker, more localizing the density gradient toward the separatrix where the negative E_r effect is dominant. All these effects make the ambient positive toroidal rotation smaller for LFS fueling than HFS fueling.

Perhaps, the more relevant quantity to consider in the L-H transition may not be the toroidal rotation itself, but the E_rxB shear which can be related to the toroidal rotation.

One relationship reported in the literature is again through the neutral effect in Refs. [6,7]. However, this relationship may be more complicated in a diverted edge due to ion orbit effect in the presence of X-point, as explained in Ref. [11]. The above XGC investigations show that the L-mode E_rxB shear is greater for the HFS midplane fueling than the LFS midplane fueling. This is consistent with the theoretical prediction in Refs. [6,7], and with the experimental observations that the H-mode transition is easier for HFS midplane fueling. The E_rxB shear becomes even greater in the H-mode simulation.

We note again that the predictions shown in Figs. 5 and 6 are qualitatively consistent with the data in Fig. 3-4, albeit with the acknowledgement that the diagnostic does not presently have the spatial resolution to measure the radial structure of the predicted velocity. On final point to note was that the numerical results in fig. 5-6 represent main ion rotation, whereas the measurements were for the C2+ ion. Previous experiments [14] in DIII-D helium discharges have shown that the impurity rotation could be different from the main ion rotation. Hence a set of XGC code calculations was done which confirmed that, for the NSTX edge conditions, the C2+ rotation had qualitatively the same relative changes as the deuterium to the gas fueling location and the L-mode vs. H-mode final state. In those calculations the carbon 2+ was introduced as a trace impurity ion in the fixed background plasmas obtained from each of the three previous XGC calculation of main ion transport. Note that these simulations do not attempt to explore the dynamics of the transition itself, but rather the pre- and post-transition states.

In summary, we have conducted experiments to test the effect of gas injector location on H-mode access and quality. We find that HFS midplane fueling leads to the most reproducible access in lower-single null discharges with an obviously lower L-H threshold power. The edge rotation measurements are qualitatively consistent with an analytic theory and Monte Carlo transport calculations. In double-null configuration, H-mode access is equally well achieved by HFS midplane or HFS top corner injection, which may be due to improved trapping of gas along the inboard boundary in double-nulls.

This experiment, combined with a theoretical modeling, is clearly only a first step to understanding the effect of the fueling location on H-mode access and power thresholds, and it is clear that additional work is required in several areas. For example, we note that the edge rotation prior to the transition is in the co-I_p direction and it reverses strongly after the L-H transition. In other words the LFS fueling produced a less positive edge rotation, which is closer to the final negative rotation in the H-mode state. Hence it appears that the important parameter is probably not the rotation itself, but probably its gradient as discussed earlier in relation to the ExB shear close to the separatrix. An upcoming experiment will investigate specifically this point.

In addition, the degree to which the poloidal dependence of the fueling source can be affected by the gas puff location, however, requires extensive neutral density measurements. At a minimum the neutral density distributions need to be measured at the inner and outer midplanes, as well as the X-point regions. Such measurements would allow an assessment of the importance of local and main chamber recycling/fueling, as compared with divertor fueling in the vicinity of the X-point regions.

Acknowledgements

This research was supported by US D.O.E. contracts DE-AC05-00OR22725, DE-AC02-76CH03073, W-7405-ENG-36, and grants DE-FG02-99ER54524, DE-FG02-99ER54519 and DE-FG02-99ER54523. We gratefully acknowledge the contribution of the NSTX technical staff and neutral beam operations staff.

Figure captions

1 – gas injector locations in NSTX.

2 – visible light emission (unfiltered) during fueling from different poloidal locations. Circles highlight the regions of enhanced emission.

3 – comparison of discharges fueled from the HFS midplane (black-solid), the outboard side (blue-dashed), and HFS top (orange-dash-dot). All discharges had the same NBI timing. The gas flow rate time dependence (b) is slightly different for the HFS top injector, but the total gas input (c) is well matched. The line average electron density from Thomson Scatterring (d) is comparable in all discharges near the time of the L-H transition, as is the loss power P_{LOSS} flowing through the separatrix (e). The HFS top and LFS fueling discharges did not undergo an L-H transition, as shown in the D_{α} (f).

4 – *comparison of edge toroidal rotation for discharges fueled from fig. 3: the HFS midplane (black-solid and green-dash-dot-dot), the outboard side (blue-dashed), and HFS top (orange-dash-dot). The edge rotation was marginally higher for the HFS midplane discharge which exhibited an H-mode transition (time indicated by the vertical bar). Data in the vicinity of large ELMs and reconnections are not plotted because the boundary shape is affected, changing the relation between the vieweing chord and the separatrix.*

5 – comparison of predicted toroidal rotation with HFS midplane (inside) and LFS (outside) fueling with the XGC code.

6 – comparison of predicted toroidal rotation in H-mode and L-mode phases of HFS midplane fueling with the XGC code.

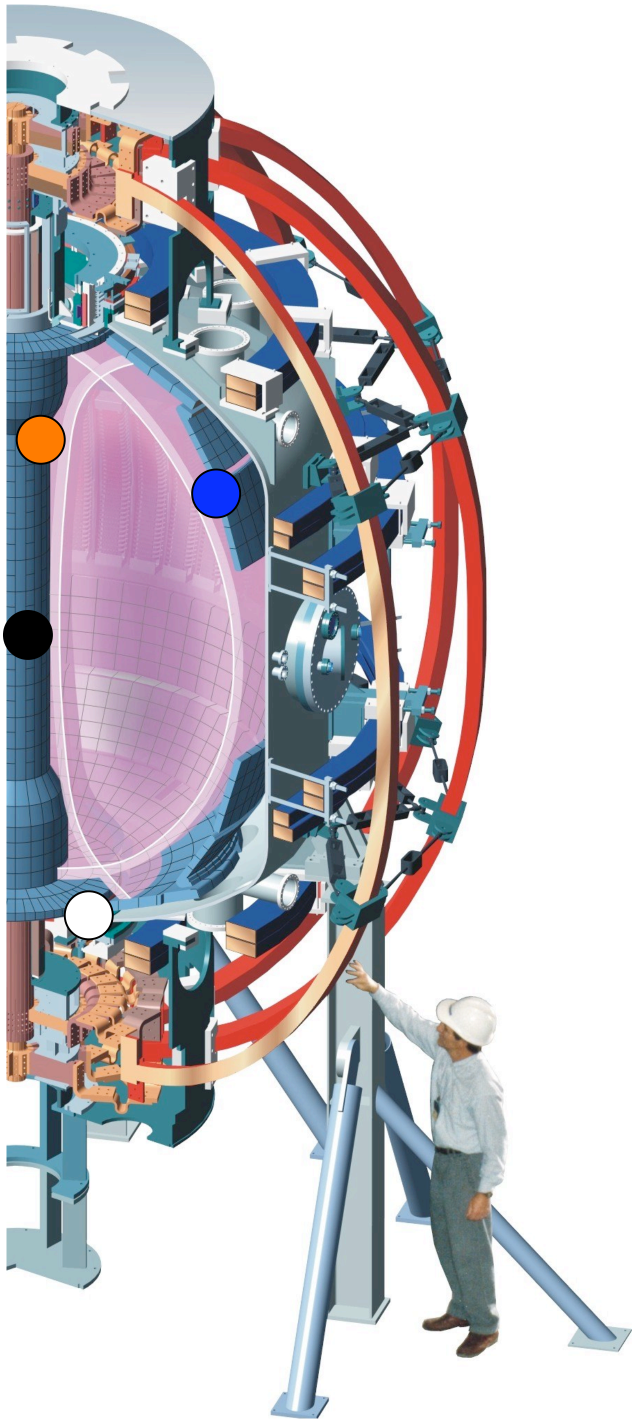

Fig. 1

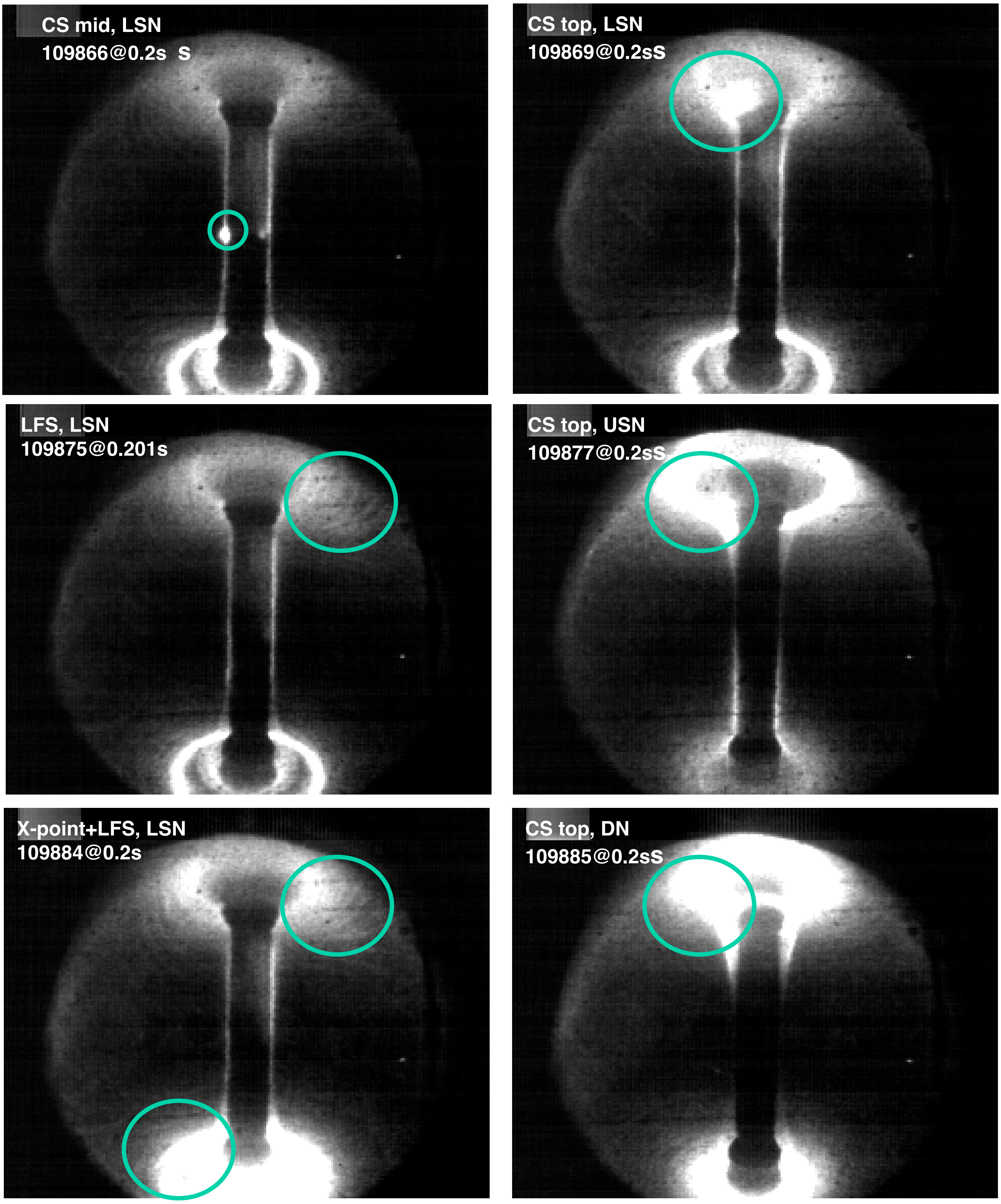
CS mid, LSN
109866@0.2s S
CS top, LSN
109869@0.2sS
LFS, LSN
109875@0.201s
CS top, USN
109877@0.2sS
X-point+LFS, LSN
109884@0.2s
CS top, DN
109885@0.2sS

Fig. 2

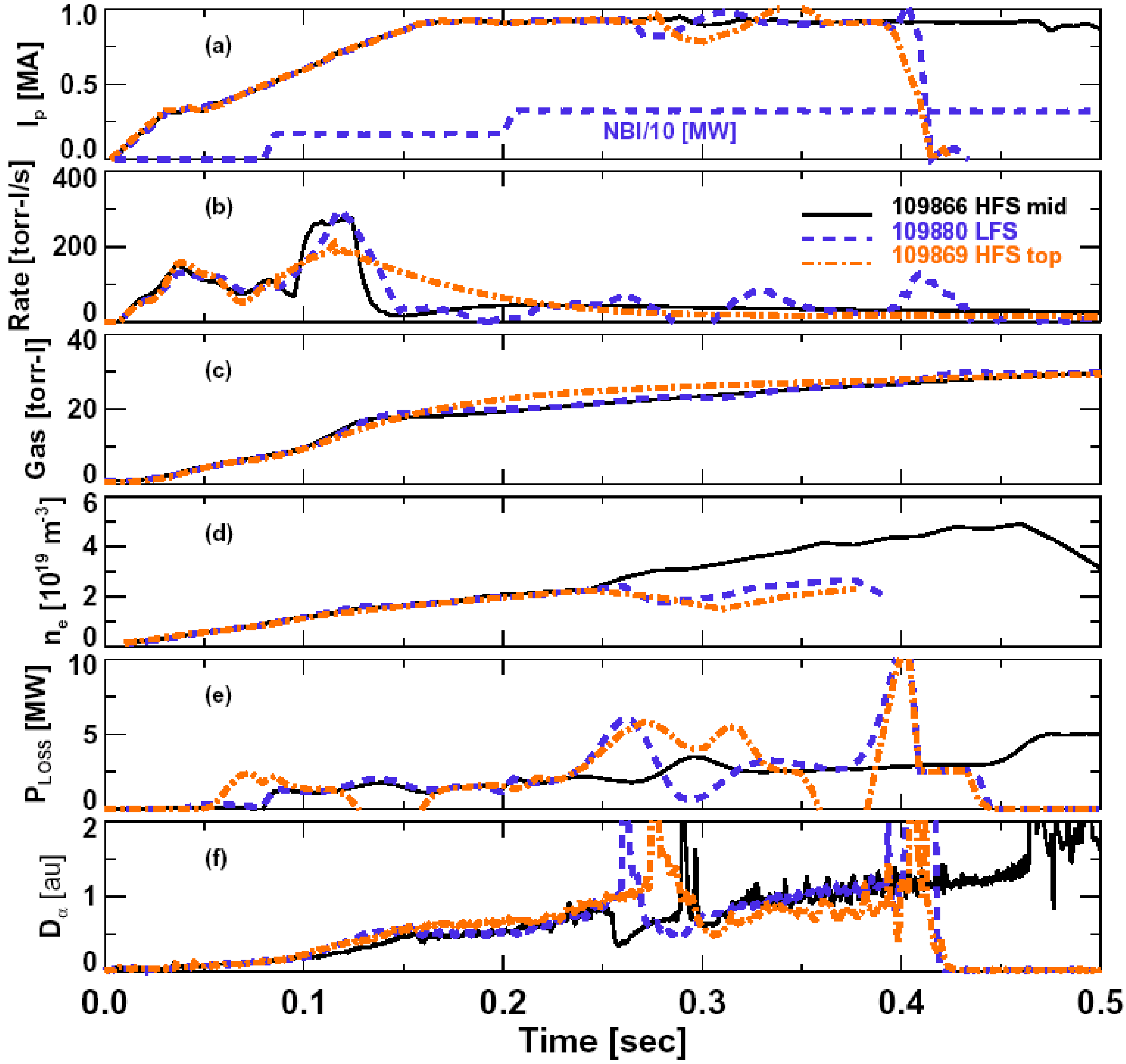

(a)
(b)
(c)
(d)
(e)
(f)
1.0
0.5
0.0
I_p [MA]
NBI/10 [MW]
400
200
0
Rate [torr-l/s]
109866 HFS mid
109880 LFS
109869 HFS top
40
20
0
Gas [torr-l]
6
4
2
0
n_e [10^{19} m^{-3}]
10
5
0
P_{LOSS} [MW]
2
1
0
D_α [au]
0.0
0.1
0.2
0.3
0.4
0.5
Time [sec]

Fig. 3

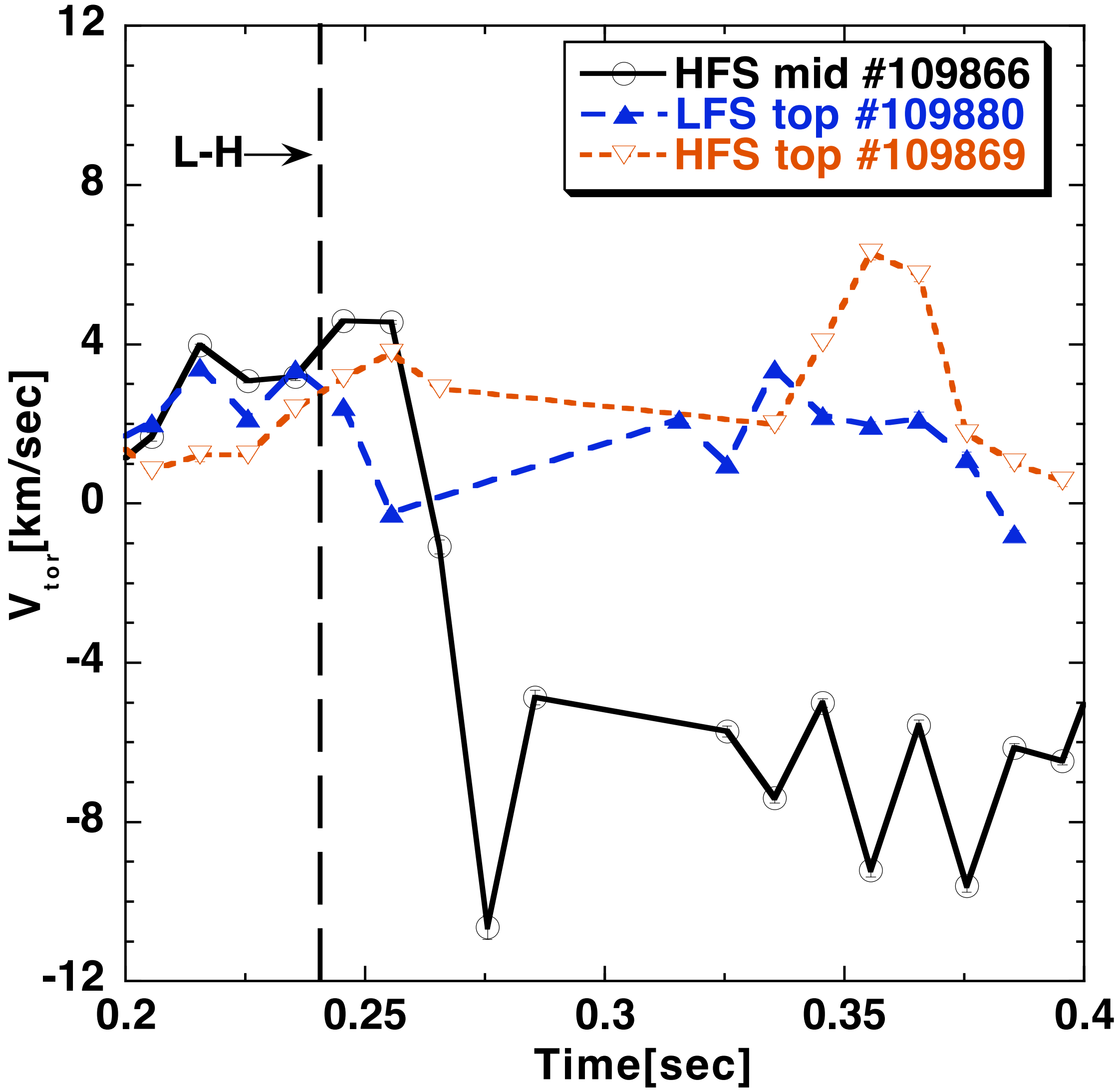

HFS mid #109866
LFS top #109880
HFS top #109869
L-H
12
8
4
0
-4
-8
-12
V_tor[km/sec]
0.2
0.25
0.3
0.35
0.4
Time[sec]

Fig. 4

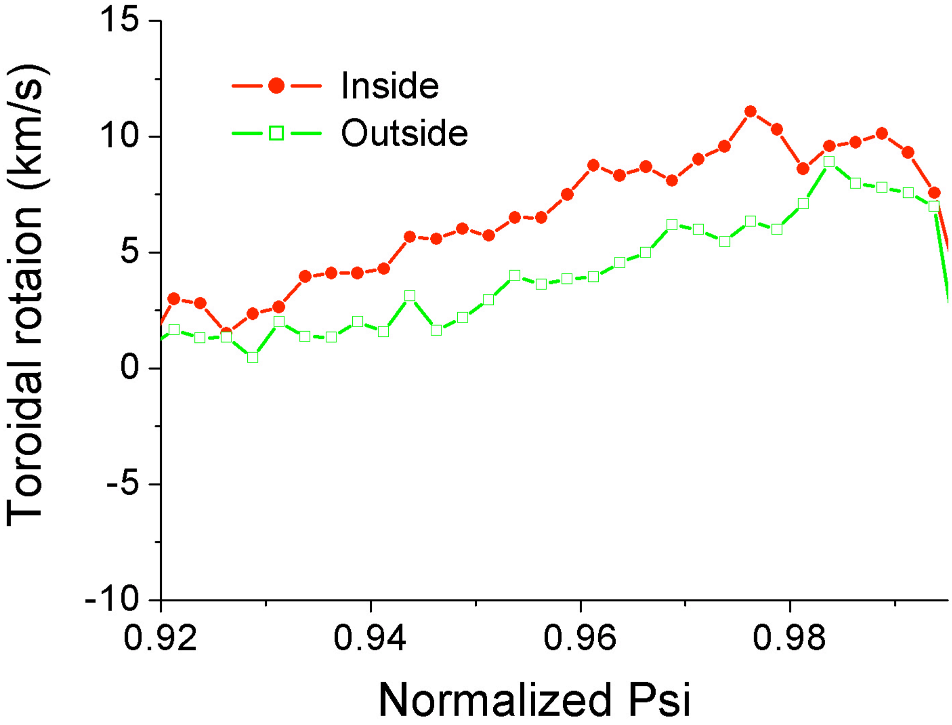

15
10
5
0
-5
-10
Toroidal rotaion (km/s)
Inside
Outside
0.92
0.94
0.96
0.98
Normalized Psi

Fig. 5

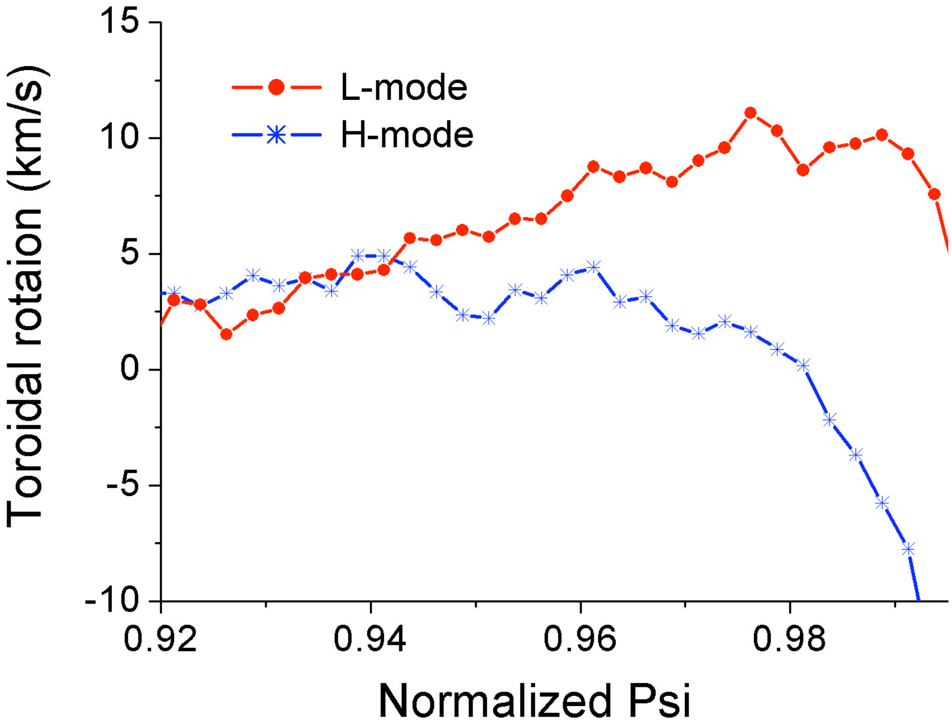

15
10
5
0
-5
-10
0.92
0.94
0.96
0.98
Toroidal rotaion (km/s)
Normalized Psi
L-mode
H-mode

Fig. 6

References

[1] A.R. Field, et. al., *Plasma Phys. Contr. Fusion* **44** (2002) A113.
[2] R. Maingi, et. al., *Nucl. Fusion* **43** (2003) 969.
[3] M. Valovic, et. al., *Plasma Phys. Contr. Fusion* **44** (2002) A175.
[4] L.R. Baylor, et. al., *J. Nucl. Mater.* **313-6** (2003) 530.
[5] H.W. Kugel, et. al., "NSTX High-Field Side Gas Fueling System", Proc. of the 2003 SOFE conference on Fusion Technology, San Diego, CA, 14-17 Oct. 2003.
[6] T. Fulop, P. Helander, and P.J. Catto, *Phys. Rev. Letts.* **89** (25 Nov. 2002) #225003;
[7] P. Helander, T. Fulop, and P.J. Catto, "Controlling Edge Plasma Rotation Through Poloidally Localized Fueling", *Phys. Plasma* **10** (2003) 4396.
[8] H.W. Kugel, V. Soukhanovskii, M. Bell, et. al., *J. Nucl. Mater.* **313-316** (2003) 187.
[9] C.E. Bush, et. al., *Plasma Phys. Contr. Fusion* **44** (2002) A323.
[10] T. Biewer, et. al., "An Edge Rotation and Temperature Diagnostic on NSTX", submitted to *Rev. Sci. Instr.*, 8/03.
[11] C.S. Chang, S.h. Ku, and H. Weitzner, "Monte Carlo Particle Simulation of Edge Pedestal and Er-Layer Formation Including Neutral Particle and Anomalous Diffusion Effects," *Phys. Plasma*, at press, 2/04.
[12] R. White, Phys. Fluids B **2** (1990) 845; A. H. Boozer, Phys. Fluids **27** (1984) 2441; R. G. Littlejohn, Phys. Fluids **28** (1985) 2015.
[13] F. L. Hinton and R. D. Hazeltine, Rev. Mod. Physics **48**, 239 (1976) 239.
[14] J. Kim, K.H. Burrell, P. Gohil, et. al., *Phys. Rev. Letts.* **72** (1994) 2199.

External Distribution

Plasma Research Laboratory, Australian National University, Australia
Professor I.R. Jones, Flinders University, Australia
Professor João Canalle, Instituto de Fisica DEQ/IF - UERJ, Brazil
Mr. Gerson O. Ludwig, Instituto Nacional de Pesquisas, Brazil
Dr. P.H. Sakanaka, Instituto Fisica, Brazil
The Librarian, Culham Laboratory, England
Mrs. S.A. Hutchinson, JET Library, England
Professor M.N. Bussac, Ecole Polytechnique, France
Librarian, Max-Planck-Institut für Plasmaphysik, Germany
Jolan Moldvai, Reports Library, Hungarian Academy of Sciences, Central Research Institute for Physics, Hungary
Dr. P. Kaw, Institute for Plasma Research, India
Ms. P.J. Pathak, Librarian, Institute for Plasma Research, India
Ms. Clelia De Palo, Associazione EURATOM-ENEA, Italy
Dr. G. Grosso, Instituto di Fisica del Plasma, Italy
Librarian, Naka Fusion Research Establishment, JAERI, Japan
Library, Laboratory for Complex Energy Processes, Institute for Advanced Study, Kyoto University, Japan
Research Information Center, National Institute for Fusion Science, Japan
Dr. O. Mitarai, Kyushu Tokai University, Japan
Dr. Jiangang Li, Institute of Plasma Physics, Chinese Academy of Sciences, People's Republic of China
Professor Yuping Huo, School of Physical Science and Technology, People's Republic of China
Library, Academia Sinica, Institute of Plasma Physics, People's Republic of China
Librarian, Institute of Physics, Chinese Academy of Sciences, People's Republic of China
Dr. S. Mirnov, TRINITI, Troitsk, Russian Federation, Russia
Dr. V.S. Strelkov, Kurchatov Institute, Russian Federation, Russia
Professor Peter Lukac, Katedra Fyziky Plazmy MFF UK, Mlynska dolina F-2, Komenskeho Univerzita, SK-842 15 Bratislava, Slovakia
Dr. G.S. Lee, Korea Basic Science Institute, South Korea
Institute for Plasma Research, University of Maryland, USA
Librarian, Fusion Energy Division, Oak Ridge National Laboratory, USA
Librarian, Institute of Fusion Studies, University of Texas, USA
Librarian, Magnetic Fusion Program, Lawrence Livermore National Laboratory, USA
Library, General Atomics, USA
Plasma Physics Group, Fusion Energy Research Program, University of California at San Diego, USA
Plasma Physics Library, Columbia University, USA
Alkesh Punjabi, Center for Fusion Research and Training, Hampton University, USA
Dr. W.M. Stacey, Fusion Research Center, Georgia Institute of Technology, USA
Dr. John Willis, U.S. Department of Energy, Office of Fusion Energy Sciences, USA
Mr. Paul H. Wright, Indianapolis, Indiana, USA

The Princeton Plasma Physics Laboratory is operated
by Princeton University under contract
with the U.S. Department of Energy.

Information Services
Princeton Plasma Physics Laboratory
P.O. Box 451
Princeton, NJ 08543

Phone: 609-243-2750
Fax: 609-243-2751
e-mail: pppl_info@pppl.gov
Internet Address: http://www.pppl.gov